

Figure 4. Amplitude power spectrum of KIC 11911480 from the Q12 (top) and Q16 (bottom) data. The Xs above certain frequencies indicate the *Kepler* spurious frequencies and the dashed horizontal line corresponds to the 3σ threshold limit. The values noted above each significant frequency corresponds to period (in seconds) of the given pulsation mode.

period, have been detected from the analysis of many early *Kepler* quarters. Some components in the power spectrum of KIC 11911480 appear and disappear between both quarters and it is clear that the amplitudes of the detected frequencies are generally stronger in Q16 than in Q12 (see Fig. 5). The error on the amplitudes is 0.028 per cent. This large overall amplitude variation between Q12 and Q16 may be explained by the fact that our target was observed with two different custom masks in both quarters.

We calculate the frequencies and amplitudes of each significant peak, using a least-squares sine wave fitting routine at each individually selected peak from the FT. We find seven pulsation modes detected above the 3σ threshold in the Q16 data set, four of which are independent (Table 2). In the Q12 data, we find five pulsation modes above the 3σ threshold, out of which three are independent. The pulsation modes found in Q12 are all detected in Q16 as well. In Table 2, we also add two pulsation periods, f_5 and $f_4 - f_1$, which are not significantly detected in Q12 but they are very close to the Q16 3σ threshold. Their amplitudes are larger than the $4\langle A \rangle = 0.099$ per cent for Q16. The main reason we believe in the detection of f_5 is because it shows splitting with the same frequency separation as the other significant modes. Also, $f_4 - f_1$ is a non-linear combination of two significant frequencies. In total, we find that KIC 11911480 has five independent pulsation modes and four combination frequencies. Non-linear combination frequencies are not generated by the same physical mechanism driving the pulsations of the star. Brickhill (1992) showed that these combination frequencies may

come from the distortion of the sinusoidal waves associated with the normal modes travelling from the convective to the radiative zone of the star, where the heat transport changes dramatically at the base of the hydrogen ionization zone (see also Wu & Goldreich 1999; Vuille 2000; Wu 2001; Yeates et al. 2005). Their amplitudes can provide information on the physical conditions in the WD convection zone (Montgomery 2005).

Also, we look into the phases of these modes and find that they are coherent enough to produce an O–C diagram over the 15-month *Kepler* observations but are indicative of a large drift in phase. We will address the analysis of those phase changes in a future paper as this requires a careful treatment of the Q12 and Q16 data obtained with different pixel masks.

We also notice splitting of some of the modes, which are denoted with ‘+’ or ‘–’ signs and placed next to the central component (‘o’) of each pulsation mode in Table 2. Not all components of a multiplet are always detected (see Fig. 5). A full asteroseismic study is beyond the scope of this paper, yet we have attempted to match the observed periods to adiabatic pulsation models with the constraints provided by our spectroscopic mass and temperature determinations. The models of Romero et al. (2012) of a $0.57 M_{\odot}$, 12 101 K WD with a thick ($10^{-3.82} M_{\text{WD}}$) hydrogen layer mass are in decent agreement with the observed periods of $f_1 - f_4$ if these four modes have $\ell = 1$ and $k = 4, 3, 5, 2$, respectively. However, this is only qualitative guess at a solution, and a full asteroseismic analysis is required to arrive at a more secure identification of these modes.

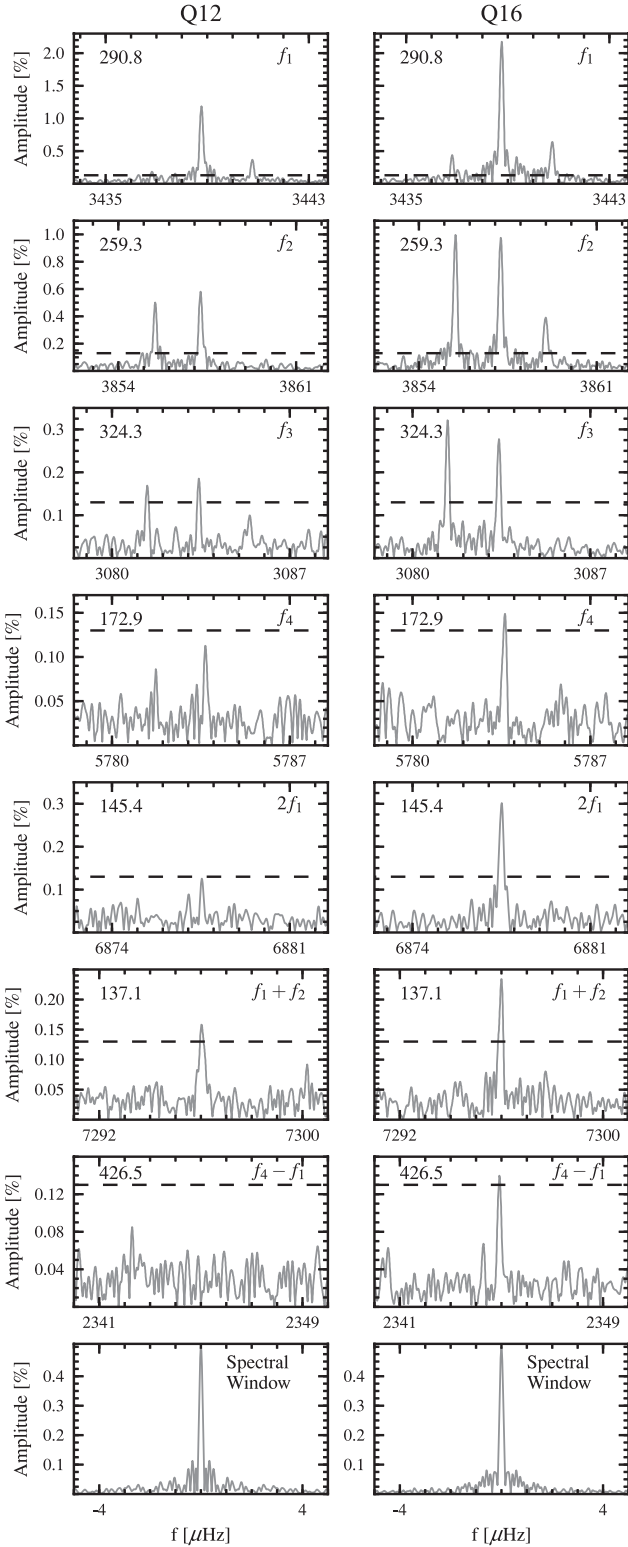


Figure 5. *Kepler* amplitude power spectra of KIC 11911480, our first ZZ Ceti discovered in the *Kepler* field from KIS. The panels on the left correspond to the Q12 data, whereas the ones on the right correspond to the Q16 data. The dashed lines correspond to the 3σ significance threshold in each data set. The top left hand side of each panel shows the corresponding period (in s). The bottom panels in both columns show the spectral window of each quarter. Splitting of the modes is a direct indication of the star’s rotation (note that it is common that not all modes of a multiplet are detected at a particular epoch; see e.g. table 5 of Kepler et al. 2003).

4.3 Rotation rate

We see what appears to be multiplet splitting of some modes, which is a direct manifestation of the star’s rotation rate (Fig. 5). In the limit of slow rotation, the difference between the frequency of one mode of indices l, k, m ($\sigma_{k,lm}$) and the frequency in the non-rotating case ($\sigma_{k,l}$) is:

$$\sigma_{k,l,m} - \sigma_{k,l} = m(1 - C_{k,l})\Omega \quad (1)$$

where $C_{k,l}$ comes from the Coriolis force term in the momentum equation and Ω is the rotation frequency (Winget et al. 1991; Vauclair 1997). Note that this equation is the classical first-order expansion. In the asymptotic limit for g modes, $C_{k,l}$ only depends on the degree of the mode: $C_{k,l} \simeq \frac{1}{l(l+1)}$. When a pulsating WD rotates, each mode of degree l can be split into $2l+1$ components. We see splitting into three components in several modes in the power spectrum of KIC 11911480 (see Fig. 5), which likely corresponds to an $\ell = 1$ mode in those cases, leading to $C_{k,l} \simeq 0.5$. The frequency spacing between the split components of the modes is quite consistent, $1.93 \pm 0.10 \mu\text{Hz}$, suggesting these modes are all of the same spherical degree. This corresponds to a rotation rate of 3.0 ± 0.2 d. However, $f_1 - f_4$ (with periods from 172.9 to 324.5s) are likely low-radial-order and far from the asymptotic limit, so their $C_{k,l}$ values should not be identical, and are not exactly 0.5. If we adopt the $C_{k,l}$ values of the model from Romero et al. (2012) discussed in Section 4.2, we obtain a rotation rate of 3.5 ± 0.2 d. To best reflect the systematic uncertainties, we adopt a rotation rate of 3.5 ± 0.5 d.

Notably, the small but significant deviations in the observed frequency splittings provide additional asteroseismic information, especially useful for constraining which modes are trapped by composition transition zones (Brassard et al. 1992). The shorter-period g modes have lower radial order, and these splittings are observed to have values of $1.97 \mu\text{Hz}$ for f_1 , $1.77 \mu\text{Hz}$ for f_2 , $2.03 \mu\text{Hz}$ for f_3 and $1.94 \mu\text{Hz}$ for f_4 .

This value is in agreement with previous rotation frequencies found in ZZ Ceti stars. Fontaine & Brassard (2008) give an overview on pulsating WDs and provide the asteroseismic rotation rates of seven ZZ Ceti stars, spanning from 9 to 55 h, i.e. 0.4 to 2.3 d. In the case of non-pulsating WDs, the sharp NLTE core of the H α line in their spectra has been used in many studies to measure the projected rotation velocities of the stars (Heber, Napiwotzki & Reid 1997; Koester et al. 1998; Karl et al. 2005). In all cases, the same conclusion was drawn: isolated WDs are generally *slow rotators*.

5 CONCLUSION

We report on the discovery of the second ZZ Ceti in the *Kepler* field: KIC 11911480. It was discovered using colour selections from the *Kepler*-INT Survey and confirmed with ground-based time series photometry from the RATS-*Kepler* survey. Follow-up *Kepler* short-cadence observations during Q12 and Q16 are analysed: five independent pulsation modes, as well as four non-linear combinations, were detected in the combined power spectrum of KIC 11911480, all ranging from 137.1 s to 519.6 s. The splitting of four of the independent pulsations enables us to estimate the rotation period of the star to be 3.5 ± 0.5 d, assuming these are all $\ell = 1$ modes.

An intermediate-resolution spectrum using ISIS on the WHT and DA WD model atmosphere fits returned our ZZ Ceti’s atmospheric parameters: $T_{\text{eff}} = 12\,160 \pm 250$ K and $\log g = 7.94 \pm 0.10$. This places KIC 11911480 close to the blue edge of the empirical